Supplementary Information for

A Recyclable Dynamic Semiconducting Polymer consisting of Pauli-Paramagnetic Diradicaloids Promoted and Stabilized by Catechol-Boron coordination

Youbing Mu[1]*, Chenxi Xiong[1], Minghui Cui[2], Mingxu Sun[1], Xinyu Chen[1], Hongqian Sang[1], Biao Xiao[1], Zhenxing Wang[3], Hangxu Liu[4], Zhenggang Lan[4], You Song[2]* and Xiaobo Wan[1]*

[1] Key Laboratory of Flexible Optoelectronic Materials and Technologies, Ministry of Education, School of Optoelectronic Materials & Technology, Jianghan University, Wuhan 430056, P. R. China.

[2] State Key Laboratory of Coordination Chemistry, School of Chemistry and Chemical Engineering, Nanjing University, Nanjing 210023, P. R. China.

[3] Wuhan National High Magnetic Field Center & School of Physics, Huazhong University of Science and Technology, Wuhan 430074, P. R. China.

[4] SCNU Environmental Research Institute, Guangdong Provincial Key Laboratory of Chemical Pollution and Environmental Safety & MOE Key Laboratory of Environmental Theoretical Chemistry, School of Environment, South China Normal University, Guangzhou, 510006, China.

*E-mail: muyb@jhun.edu.cn; yousong@nju.edu.cn; wanxb@jhun.edu.cn

Table of contents

1. Instruments

The ^{1}H NMR and ^{13}C NMR spectra were recorded in solution of $CDCl_3$ or DMSO-d_6 on Bruker AVANCE III HD 400/600 spectrometer (Bruker, Germany). FT-IR spectra were measured using IR Tracer-100 Fourier infrared spectrometer (SHIMADZU, Japan). Elemental analysis of the polymers was performed on an AXIS-SUPRA+ x-ray photoelectron spectrometer (XPS) (SHIMADZU, Japan). The UV-vis spectra of the monomers and polymers was tested using the PerkinElmer Lambda 1550-WB UV-vis spectrophotometer. The Young's modulus of the P(ID-O-B) film is calculated from the stress-strain curve output from the tensile transducer (LTS-50GA, KYOWA, Japan) The thicknesses of the films were obtained on a step profiler (Bruker, Germany). The relative molecular weights of the polymers were tested on a high-temperature gel permeation chromatography (HT-GPC) (Agilent, Infinity PL220, USA) at 150 ºC, using trichlorobenzene as the eluent and mono-dispersed polystyrene as the standard. Crystallinity characterization was performed on an X-ray diffractometer (X'Pert Powder, Panalytical, Netherlands). The crystal structure and orientation of P(ID-O-B) film were tested on X-ray small-angle scattering/wide-angle scattering instruments (Xeuss 3.0, Xeuss S.A.S, France). Thermogravimetric analysis of the polymer were conducted on a thermogravimetric analyzer (TG 209 F3, Netzsch, Germany), with the test temperature range from 40 to 600 ℃ and the heating rate of 20 ℃/min. The glass transition temperatures of the polymers were carried out on a differential scanning calorimeter (DSC Q-20, TA, USA) in the range of 40-350 °C under nitrogen atmosphere with a heating rate of 10 °C/min. Variable temperature electron paramagnetic resonance (VT-EPR) spectra were measured on an X-band continuous wave electron paramagnetic resonance spectrometer EPR200-Plus (CIQTEK, China). Temperature-dependent magnetization of polymers tested using a superconducting quantum interference device (SQUID) VSM magnetometer (Quantum Desigh, USA).

Film thickness test

P(ID-O-B) solution at a concentration of 5.0 mg/mL was dynamically spin-coated on clean glass slides at 2000 rpm and annealed at 150 °C for 15 minutes. The film was gently scribed with a knife to make three distinct lines, and the thickness of the film at three different locations was measured with a step profiler, and the calculated average value was taken as the actual thickness of the film.

Mechanical property test

A layer of PEDOT was spin-coated on a glass slide of 8 mm width and 15 mm length, and then annealed at 150 °C for 15 min. The PEDOT layer was then dynamically spin-coated with a P(ID-O-B) solution at a concentration of 5 mg/mL at 2000 rpm, and annealed at 150 °C for 15 min. The sample was placed flat on the surface of the water and the P(ID-O-B) film detaches from the glass slide and floats on the water surface as PEDOT gradually dissolves in the water, where the surface tension of the water flattens the film. The sensing head of the stretch sensor is positioned horizontally close to the ends of the film, to which the film is adhered by Van der Waals forces and stretched at a uniform speed of 0.1 mm/s. The stress-strain graph is drawn from the data of the tensile transducer, the slope of which is the Young's modulus of the material.

Electric property measurement

The conductivity of P(ID-O-B) was tested by *I-V* characteristics with device structure: ITO/P(ID-O-B)/Ag (100 nm). P(ID-O-B) layer was spin-coated on the ITO substrate at 2000 rpm for 40 s with the concentration of 5 mg/mL in DCM, then annealed at 150 °C for 5 minutes. At last, 100 nm of Ag was deposited by thermal evaporation under a pressure of 5×10^{-4} Pa. The *I-V* characteristics of their devices are measured by means of a probe bench and their data are output by a parameter analyzer, the conductivity of P(ID-O-B) is calculated using the following equation at last.

$$\sigma = \frac{I \times L}{U \times A}$$

(σ unit: S/cm; L: conductor film thickness; A: electrode area)

SQUID Measurement

Magnetic measurements were conducted using a SQUID VSM magnetometer. (χ-T): To rule out the interference of impurities (possible solvent or other small molecules encapsulated in the polymer), the polymer was annealed at 200 ºC to constant weight before the measurement. The direct current (dc) magnetism properties of **P(ID-O-B)** were studied in the range of 1.8-360 K at 1000 Oe. The diamagnetic contributions of the sample holders and the atoms were corrected with blank holders and the Pascal's constants. Molar magnetic susceptibility was calculated on the basis of counting one diradicaloid in every two ID units.

2. Calculation Methods

2.1. EPR simulation

To simulate the EPR spectra, we utilized the following Hamiltonian:

$$\hat{H} = g\mu_B \hat{\mathbf{S}} \cdot \mathbf{B} + D\hat{S}_z^{\,2} + E(\hat{S}_x^{\,2} - \hat{S}_y^{\,2}) \qquad (1)$$

where S is the electron spin, g is the Landé factor, D is the axial zero-field splitting (ZFS) parameter, E is the transverse ZFS parameter, μ_B is the Bohr magneton, and B is the Zeeman magnetic field. The computational spectral simulations were performed on the program SPIN developed by Andrew Ozarowski in the National High Magnetic Field Laboratory in Tallahassee, FL, USA.

2.2. DFT calculation

2.2.1. The calculation for the triplet state of the simplified model I.

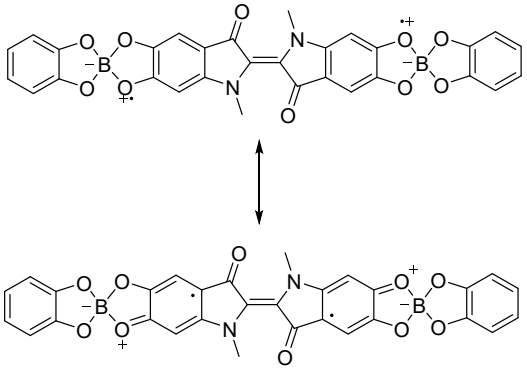

Computational Details

To verify the electronic structures shown in Figure 1, the DFT method at the ωB97XD/6-311G(d) level was chosen to optimize the geometries of both singlet and triplet states, and the symmetry breaking was considered. The results show that the lowest-state is T_1 and the corresponding geometry was labeled as Stru_T. We characterized the electronic structure of the singlet state at Stru_T by using the spin-projected unrestricted ωB97XD functional with the symmetry breaking correction. The electronic character of the current system was analyzed using the biradical character index, y, namely:

$$y = 1 - \frac{2T}{1+T^2},$$

where T is obtained from the highest occupied natural orbital (HONO) and the lowest

unoccupied natural orbital (LUNO) by the following operation:

$$T = \frac{n_{HONO} - n_{LUNO}}{2},$$

where n_{HONO}/n_{LUNO} is the occupation number of natural orbitals. The value range of y is between 0 (closed shell) to 1 (biradicals)[1]. All above calculations were performed using Gaussian 16 program package[2].

Next the single-point calculations at the Stru_T geometry were performed using spin-flip TDDFT method at the ωB97XD/6-311G(d) level. The wavefunction of the triplet state was taken as the reference and the spin flip excitation was performed to obtain the low-lying singlet states. All spin-flip TDDFT calculations were run using the Q-CHEM package[3].

2.2.2. Calculation for the interaction between two P(ID-O-B) tetramers

The calculation on the interaction between two tetramers were carried out using the CP2K Quickstep package1 and the PBE0-TC-LRC-ADMM hybrid density function2, 3, containing 20% HFX exchange, which was truncated at 2.5 Å. The cutoff of the finest real-space integration grid is 400Ry. The primary basis set is MOLOPT4, of TZV2P quality for C, N, O and H atoms with corresponding GSTH pseudopotentials5, 6. The auxiliary Gaussian basis for the ADMM method is cFIT3. The dispersion interactions were considered within the Grimme D3 Method7. The force convergence criterion used for geometry relaxations is 0.005 eV/ Å.

3. Synthetic Details

All reagents are purchased from commercial suppliers and used as received. Among them, 6-nitroveratraldehyde, 1.0 mol/L dichloromethane solution of boron tribromide and methyltrioctylammonium chloride were purchased from Energy Chemical (China), while others are purchased from Sinopharm Chemical (China). Anhydrous solvent is taken from the solvent purification and drying system. All experiments were conducted in a dry glassware under an argon atmosphere.

Synthetic route:

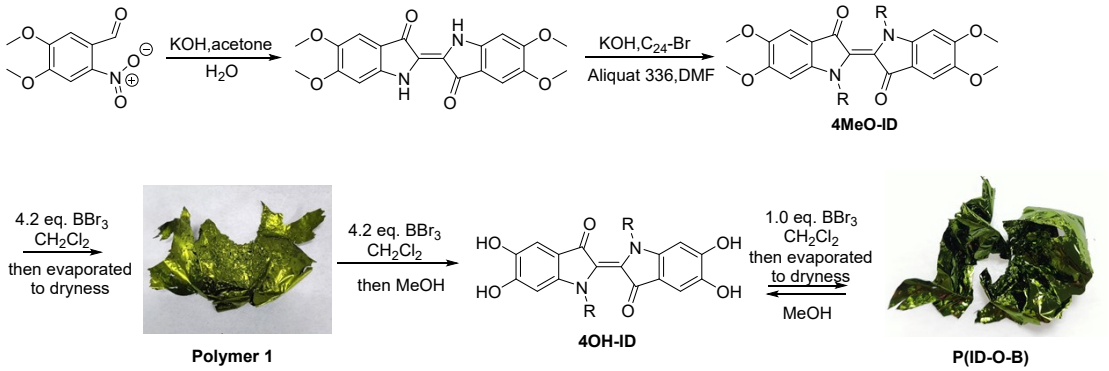

Scheme 1. Synthetic route toward the monomer 4OH-ID and polymer P(ID-O-B)

Compound 1:

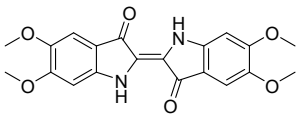

1

KOH solution (0.6 M,160 mL) was added dropwise to an acetone (500 mL) solution of 6-nitroveratraldehyde (25 g, 118.39 mmol, 1.0 eq.) at −10 °C and the color of the solution was changed from yellow to tan. Another KOH solution (0.6 M, 250 mL) was added dropwise again after 1 hour and the mixture was stirred at −10 °C for 24 hours. During this time, the color of the solution changed from tan to dark brown. After filtration under reduced pressure, the residue was washed in sequence with water, ethanol, acetone to give **compound 1** as a blue powder in 52% yield, which was directly used for next step without

further purification. Compound 1 is insoluble in common solvents and has not been characterized by ^{1}H NMR and ^{13}C NMR spectra.

4MeO-ID:

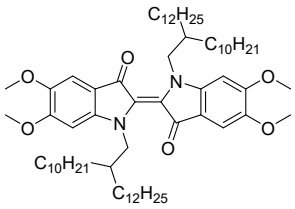

2

The mixture of **compound 1** (Supplementary Information Section 2) (2.00 g, 5.24 mmol, 1.0 eq.), Aliquat 336 (0.12 g, 0.30 mmol, 0.06 eq.), KOH (0.73 g, 13.03 mmol, 2.5 eq.), $C_{24}H_{49}$-Br (6.56 g, 15.70 mmol, 3.0 eq.) in DMF (48 mL) was refluxed at 60 ℃ for 5 hours and then quenched with saturated ammonium chloride solution (15 mL). The solvent was removed under reduced pressure and the residue was dissolved in DCM (100 mL). The resulting solution was washed three times with water (100 mL) and brine, respectively, and dried with anhydrous Na_2SO_4. After removal of the solvent, the crude product was purified by column chromatography (silica gel, PE/EA=4:1) and recrystallized with 95% ethanol solution to give a green acicular crystal in 47% yield. ^{1}H NMR (400 MHz, $CDCl_3$) δ 7.10 (s, 1H), 6.55 (s, 1H), 4.16 (d, J = 6.3 Hz, 2H), 3.98 (s, 3H), 3.87 (s, 3H), 1.84 (m, J = 5.4 Hz, 1H), 1.33 - 1.02 (m, 41H), 0.87 (t, J = 6.6 Hz, 6H); ^{13}C NMR (101 MHz, $CDCl_3$) δ 182.16, 154.85, 148.84, 143.73, 125.37, 112.37, 103.93, 93.92, 55.31, 55.22, 50.66, 34.29, 30.92, 30.90, 30.47, 29.04, 28.71, 28.66, 28.37, 28.35, 25.47, 21.68, 13.10. HRMS (ESI): calcd for $C_{68}H_{114}N_2O_6$: 1055.6680, found: 1055.8735. The ^{1}H NMR, ^{13}C NMR and mass spectra were shown in Figure S12-S14.

4OH-ID:

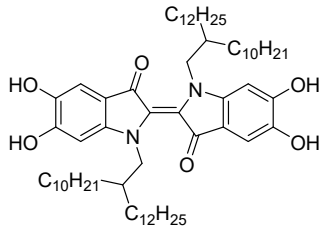

3

To a anhydrous dichloromethane (5.0 mL) solution containing **4MeO-ID** (1.00 g, 0.95 mmol, 1.0 eq.) in a 10 mL pressure tube protected with argon, was added BBr_3 solution (1 M, 4 mL, 4.2 eq.) dropwise at −78 ℃ (dry ice-acetone system) and the solution turned to blue from green. Then, the mixture was warmed gradually to room temperature and stirred overnight, and the solution became purplish-red or rose-red. The resulting mixture was transferred to a round-bottomed flask after diluting with DCM and the solvent was removed under reduced pressure. During this time, the color of the solution changed from rose-red to blue and some insoluble solids appeared after adding DCM. After being placed in environmental conditions for a period of time, the insoluble matter gradually dissolved and the solution became a purplish-red homogeneous solution. After removing the solvent, a metallic greenish film attached to the bottle wall is obtained. The film was dissolved with MeOH and a green solution can be observed. The green solution was concentrated under reduced pressure to give a gray-green powder solid, which was washed twice by DCM to yield a dark green solid (0.66 g, 70%). ^{1}H NMR (400 MHz, DMSO-d_6) δ 9.97 (s, 1H), 9.11 (s, 1H), 6.83 (s, 1H), 6.62 (s, 1H), 4.04 (d, J = 276.7 Hz, 2H), 1.65 (s, 1H), 1.07 (d, J = 38.6 Hz, 42H), 0.74 (d, J = 6.6 Hz, 6H). ^{13}C NMR (101 MHz, DMSO-d_6) δ 182.79, 154.27, 149.49, 141.19, 125.10, 112.60, 108.42, 98.63, 50.39, 34.74, 31.83, 31.27, 29.97, 29.62, 29.57, 29.29, 22.58, 14.17, 14.15. HRMS (ESI): calcd for $C_{68}H_{106}N_2O_6$: 999.8129, found: 999.8121. The ^{13}C NMR and mass spectra were shown in Figure S15 and Figure S16.

P(ID-O-B): To a suspension of **4OH-ID** (0.10 g, 0.10 mmol, 1.00 eq.) in anhydrous dichloromethane (2.0 mL) in a 10 mL pressure tube protected with argon, was added BBr_3 solution (1 M, 0.10 mL, 1.00 eq.) dropwise at −78 ℃ (dry ice-acetone system). The green-

colored suspension gradually became a blue homogeneous solution. The mixture was warmed gradually to room temperature and stirred for 24 hours, and the solution became purplish-red. Then the solvent was removed under reduced pressure, a metallic greenish film (**P(ID-O-B)**) attached to the bottle wall was obtained. The obtained film was dissolved with DCM and washed twice with water to remove bromides and dried with anhydrous Na_2SO_4. After removal of the solvent, the film can still be recovered. The ^{11}B NMR spectrum was shown in Figure S18, Supplementary Information.

4O-ID:

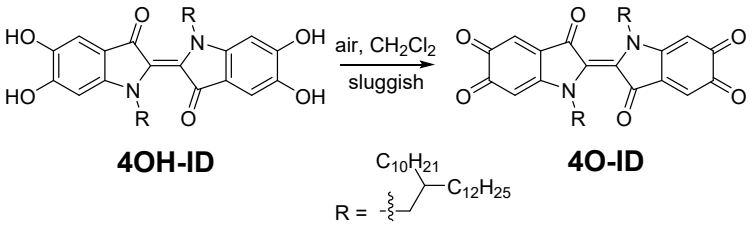

The suspension of **4OH-ID (**0.090 g) in 30 mL anhydrous dichloromethane in a 100 mL double-necked flask was refluxed at 50 ^oC under oxygen atmosphere for 3 days, and the green-colored suspension was gradually changed from a violet solution however still with remaining unreacted green-colored suspension. After filtrating the insoluble starting material, the purple-colored filtrate was collected. The solvent was removed under reduced pressure and the remaining solid product was washed with petroleum ether. After filtration, the filter residue was collected and vacuum-dried to give purple-black solid product with metallic luster (0.40 mg, 45%). No further purification was performed. The ^1H NMR spectrum of **4O-ID** was shown in Figure S17, Supplementary Information.

4. High Temperature GPC result of Polymer1&P(ID-O-B)

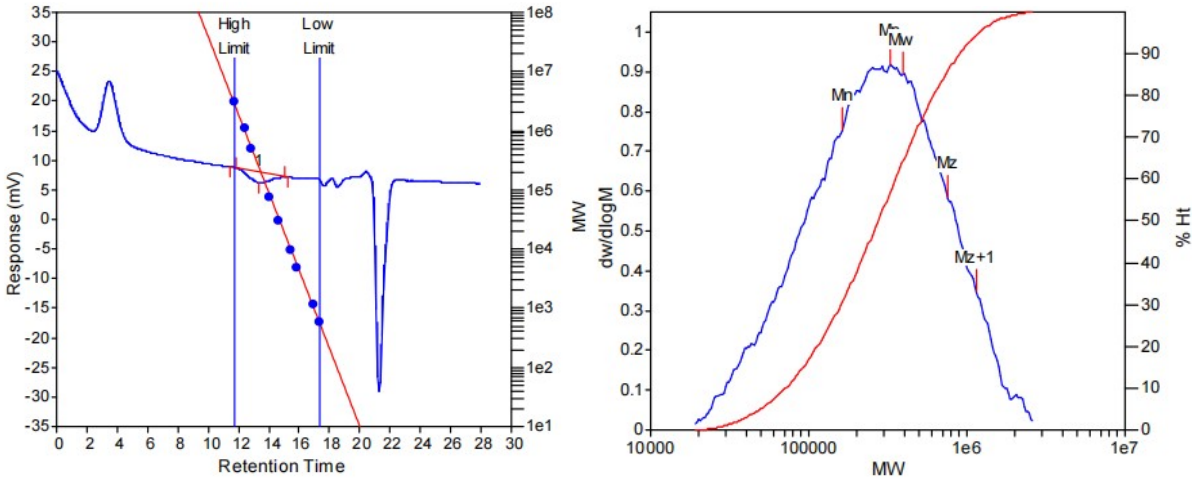

Figure S1. The left figure is chromatogram plot and the right figure is distribution plot of polymer1.

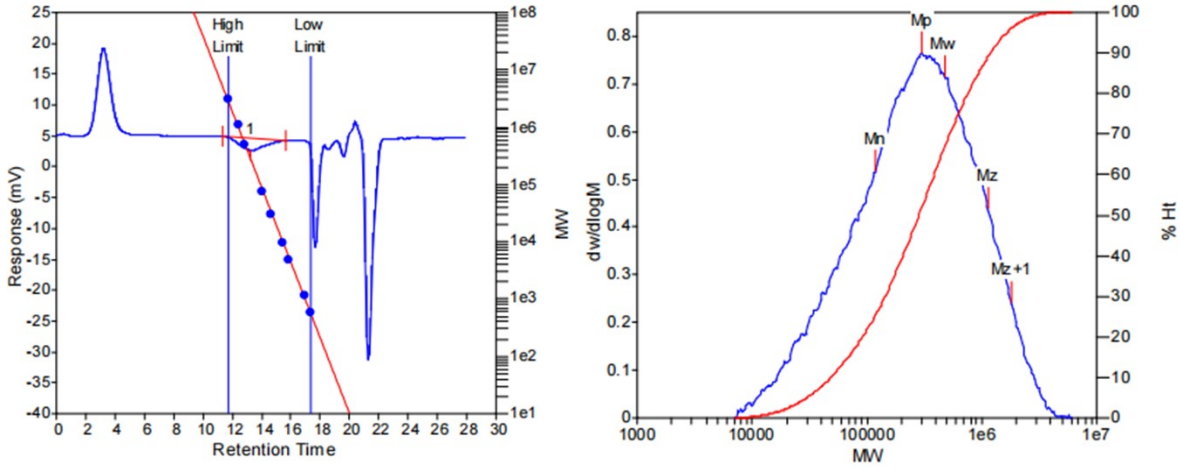

Figure S2. The left figure is chromatogram plot and the right figure is distribution plot of P(D-O-B).

Table S1. Molecular weight and dispersity **of Polymer1** and **P(D-O-B)** tested in trichlorobenzene at 150 ºC.

Name	*M*p (kDa)	*M*n (kDa)	*M*w (kDa)	*M*z (kDa)	*M*z+1 (kDa)	*M*v (kDa)	*Đ*
Polymer1	325.4	163.6	394.8	758.8	1141.1	347.2	2.41
P(ID-O-B)	301.2	119.4	477.6	1128.5	1816.5	398.3	4.00

5. XRD data for P(ID-O-B)

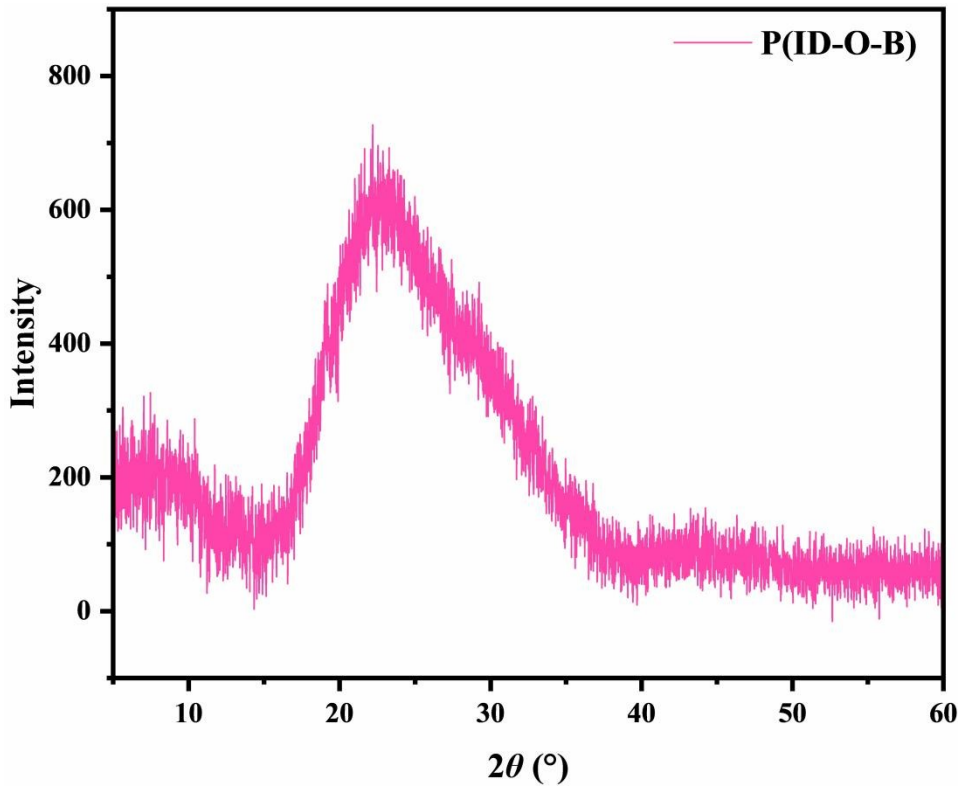

Figure S3. X-ray diffraction test pattern of P(ID-O-B) film.

Table S2. Calculation of the crystallographic spacing of P(ID-O-B).

θ (°)	d (Å)
11.19	3.97

6. Thermal performance of P(ID-O-B)&4OH-ID

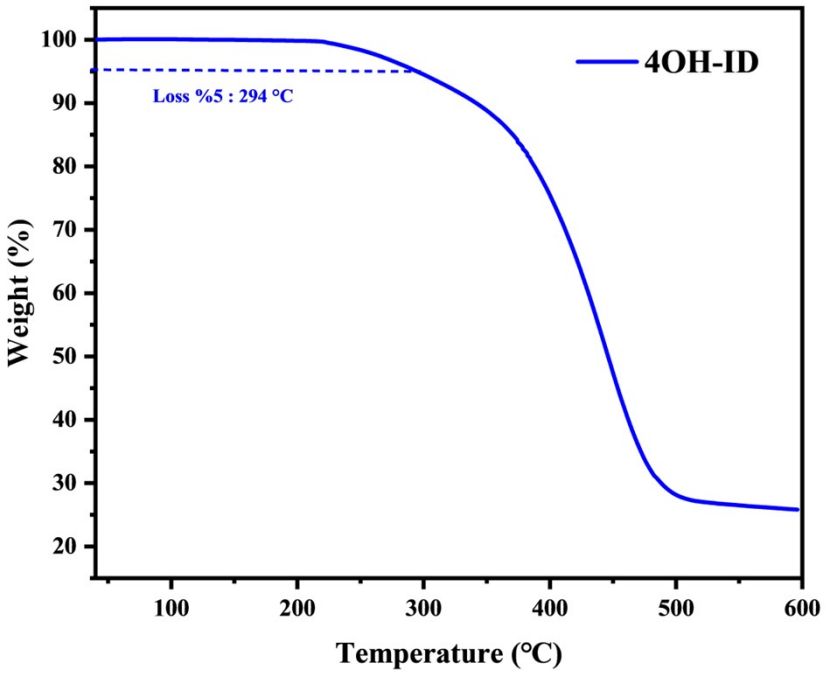

Figure S4.TGA curve of 4OH-ID.

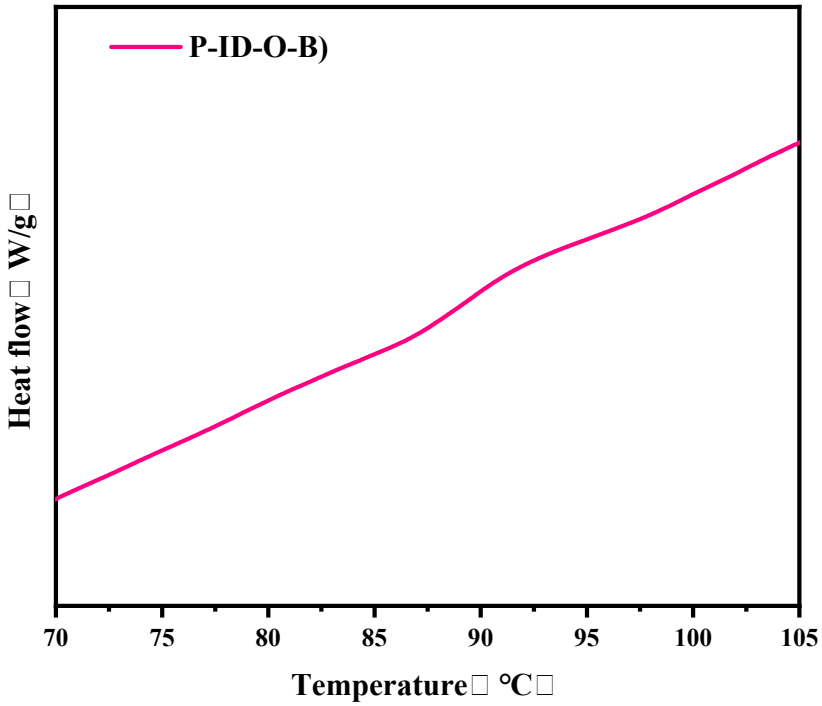

Figure S5. DSC curve of P(ID-O-B).

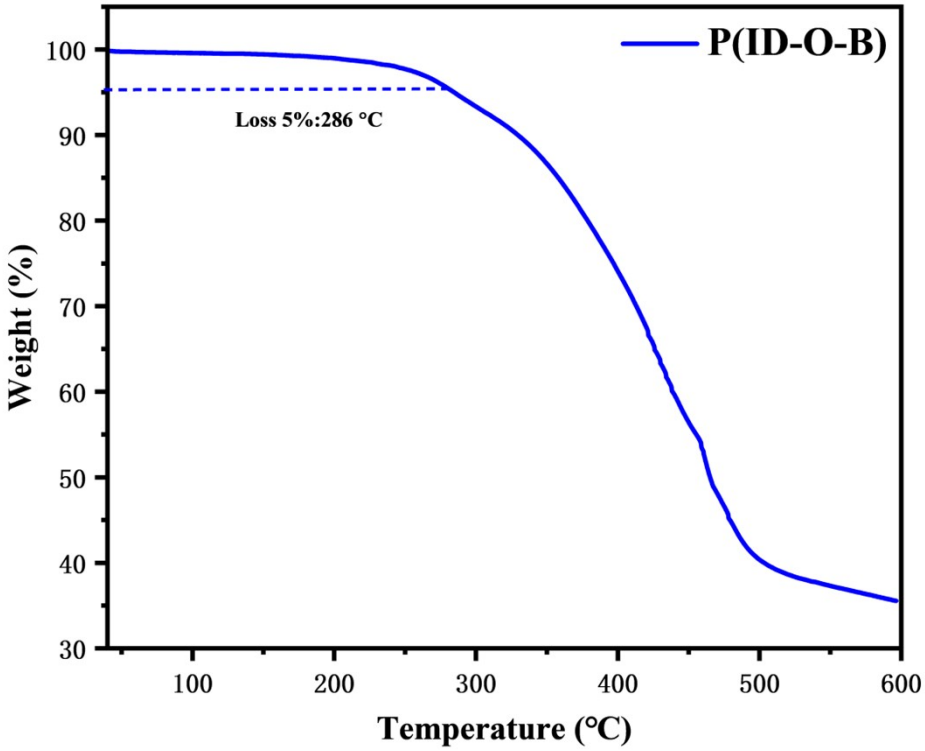

Figure S6. TGA curve of P(ID-O-B).

7. The UV-vis spectra of P(ID-O-B)

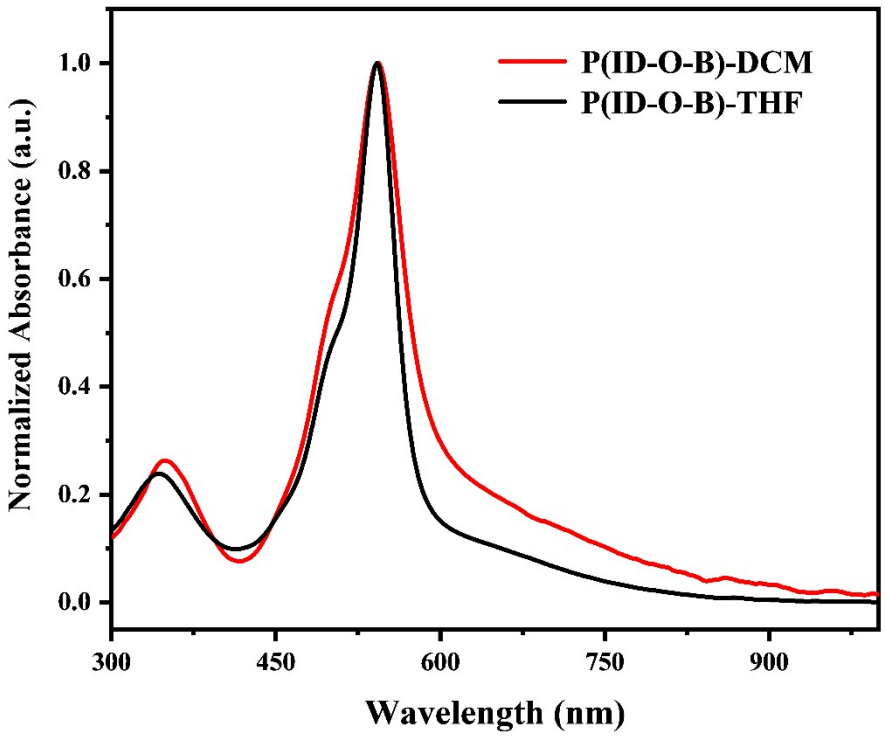

Figure S7. UV spectra of P(ID-O-B) in DCM and THF.

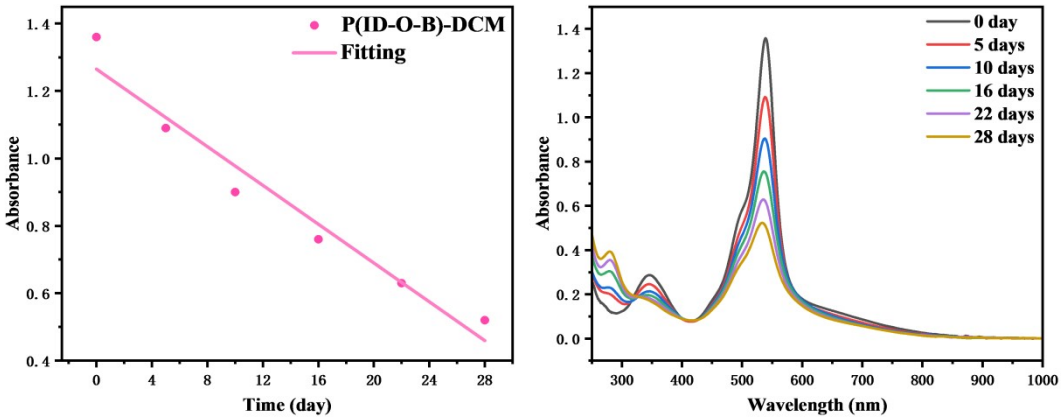

Figure S8.The half-life of the P(ID-O-B) in DCM solution.

8. Electrochemical testing for P(ID-O-B)

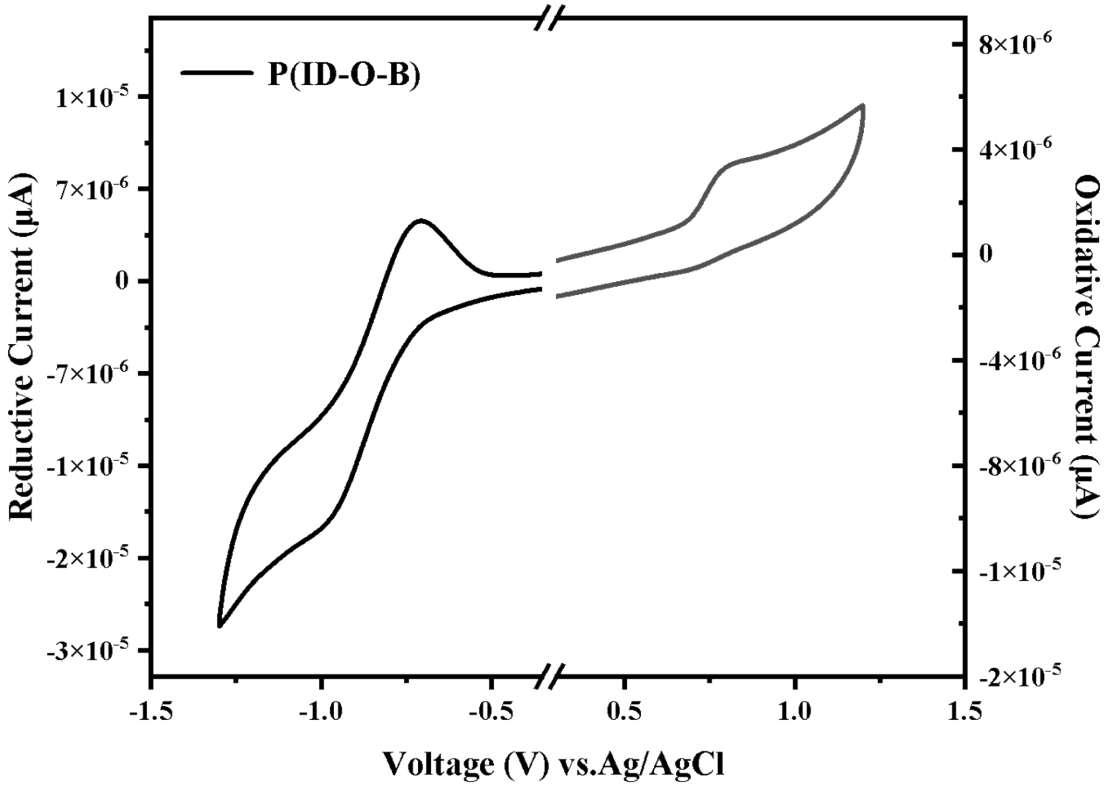

Figure S9. P(ID-O-B) Cyclic voltammogram in thin film state.

	HOMO	LUMO	E_g
eV	– 5.09	– 3.74	1.35

Table S3. Mechanical performances of P(ID-O-B) films.

9. XPS result for P(ID-O-B)

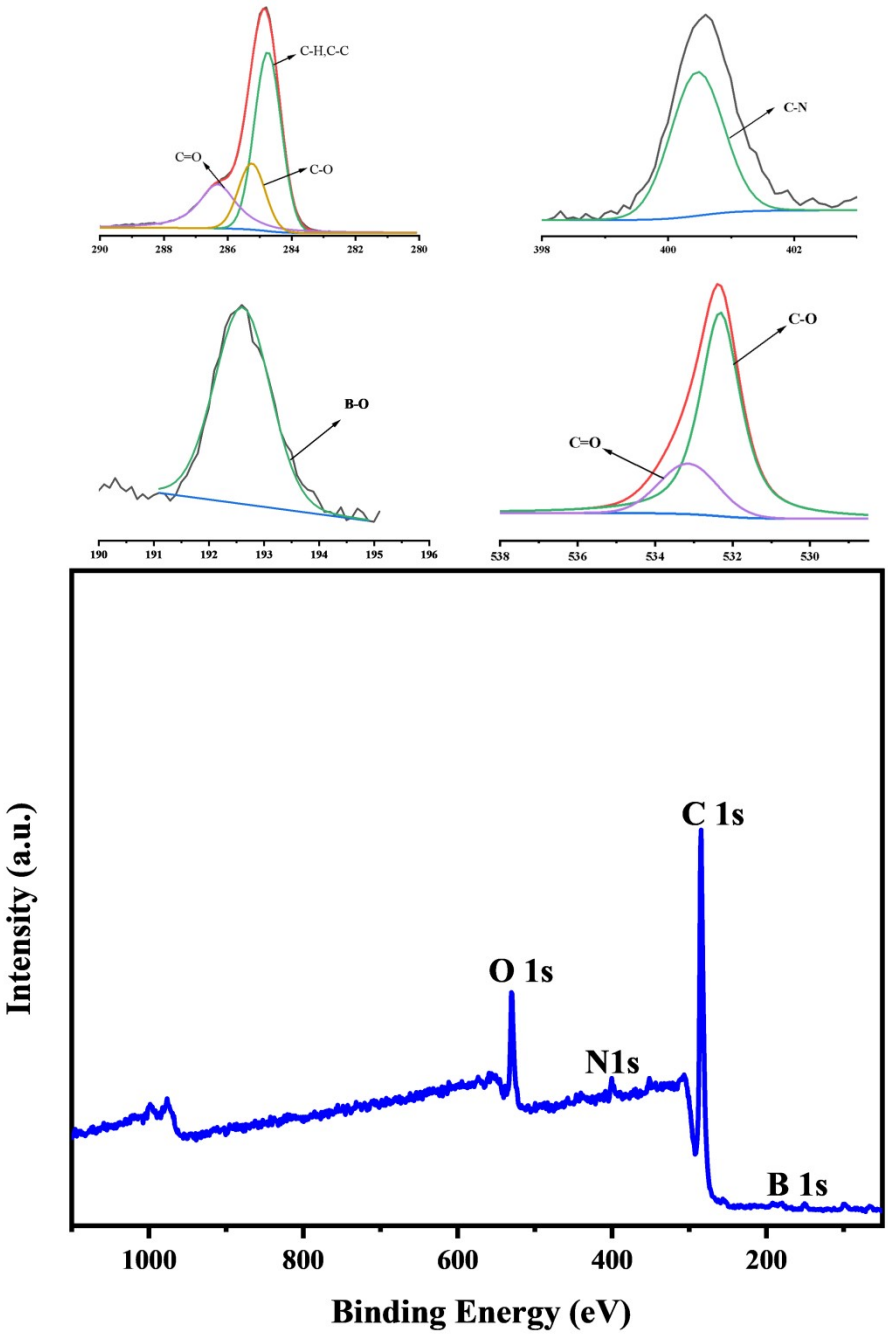

Figure S10. XPS spectrum of P(ID-O-B).

10. Film thickness test for P(ID-O-B)

Table S4. The thickness of P(ID-O-B) films.

	①	②	③	average
Film thickness	124 nm	119 nm	123 nm	122 nm

11. Mechanical performance testing for P(ID-O-B)

Table S5. Mechanical performances of P(ID-O-B) films.

	①	②	③	④	average
Elongation at break (%)	4.53	3.49	4.38	3.53	3.98
Young's Modulus (MPa)	1261	1220	1220	1221	1231

12. Electrical conductivity test for P(ID-O-B)

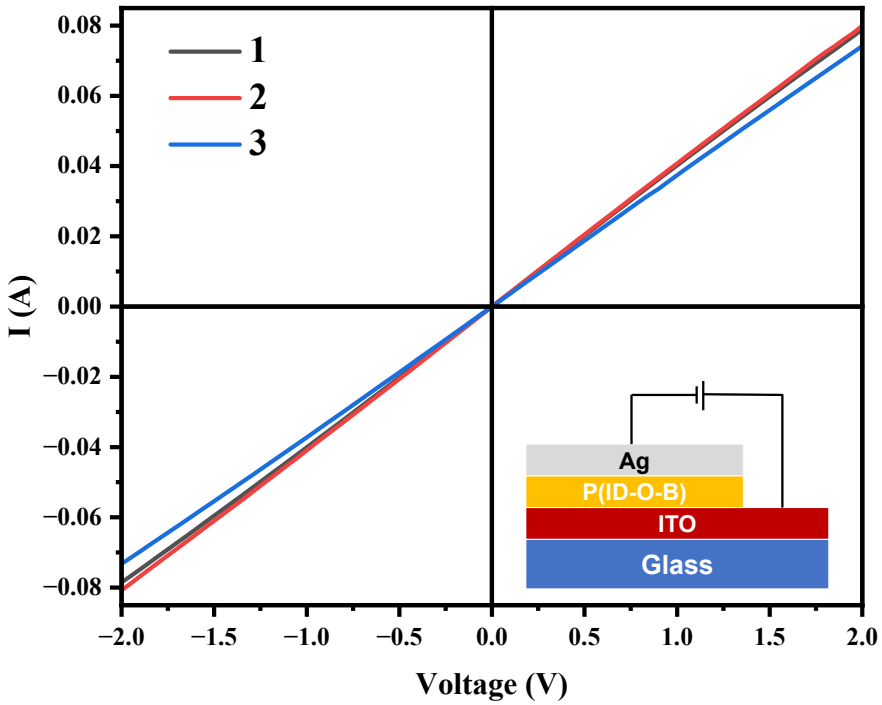

Figure S11. Device schematic and *I-V* curve for P(ID-O-B).

Table S6. The electric conductivity of P(ID-O-B) films.

	①	②	③	average
σ (S/cm)	2.29×10^{-6}	2.34×10^{-6}	2.14×10^{-6}	2.26×10^{-6}

13. Calculation of layer spacing for P(ID-O-B)

Table S7. Calculation of layer spacing for P(ID-O-B).

	q_Z(Å^{-1})	d (Å)
(100)	0.3151	19.9333
(010)	1.4446	4.34728

14. ^{1}H NMR spectra for 4OH-ID&P(ID-O-B)

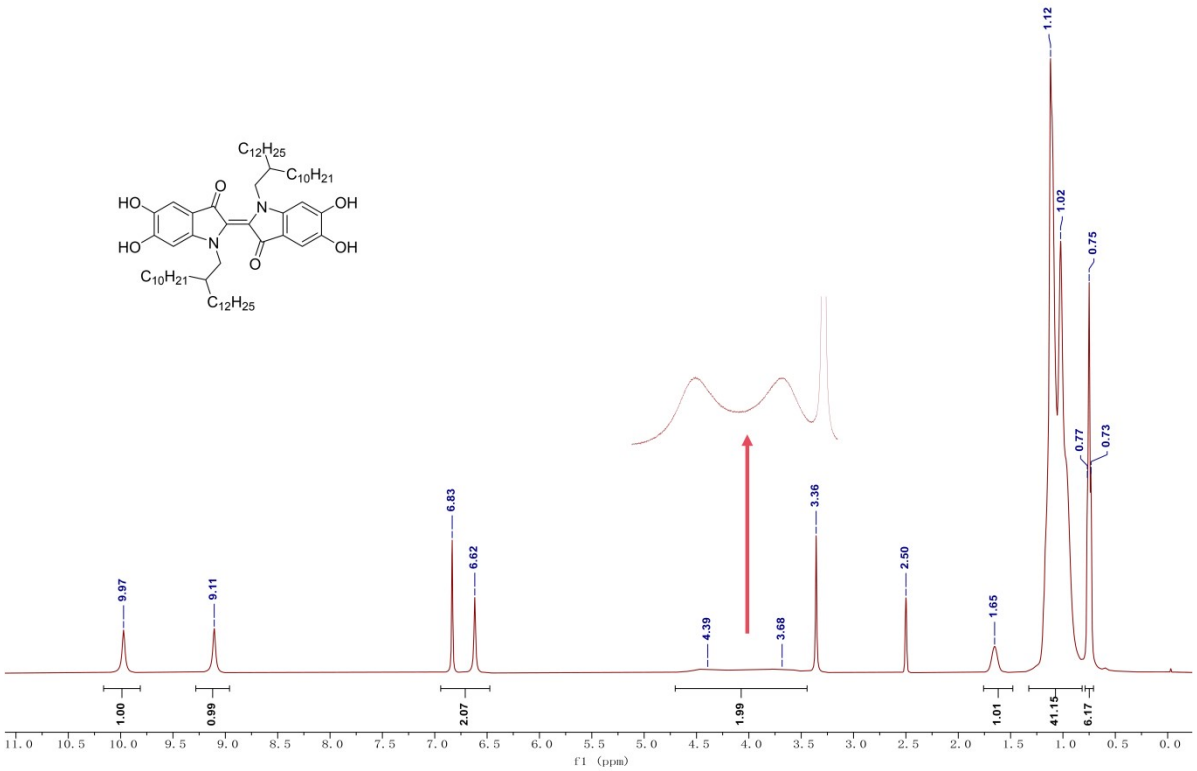

Figure S12. ^{1}H NMR spectrum (400 MHz) of compound 3 (4OH-ID) in DMSO-*d6*.
Peak assignment: (9.97 ppm and 9.11 ppm: two OH groups; 6.83 ppm: 1H, aromatic proton next to the carbonyl group; 6.62 ppm: 1H, aromatic proton next to the amine group; 4.39 and 3.68 ppm: 2H, the methylene protons next to N atom; 1.65 ppm: 1H , proton on the branch point; 1.12 and 1.02 ppm: aliphatic protons on the sidechain; 0.75 ppm: 6 H (triplet), two terminal methyl groups). Peak at 3.36 and 2.50 ppm are assigned to the residue DMSO-*d6*.

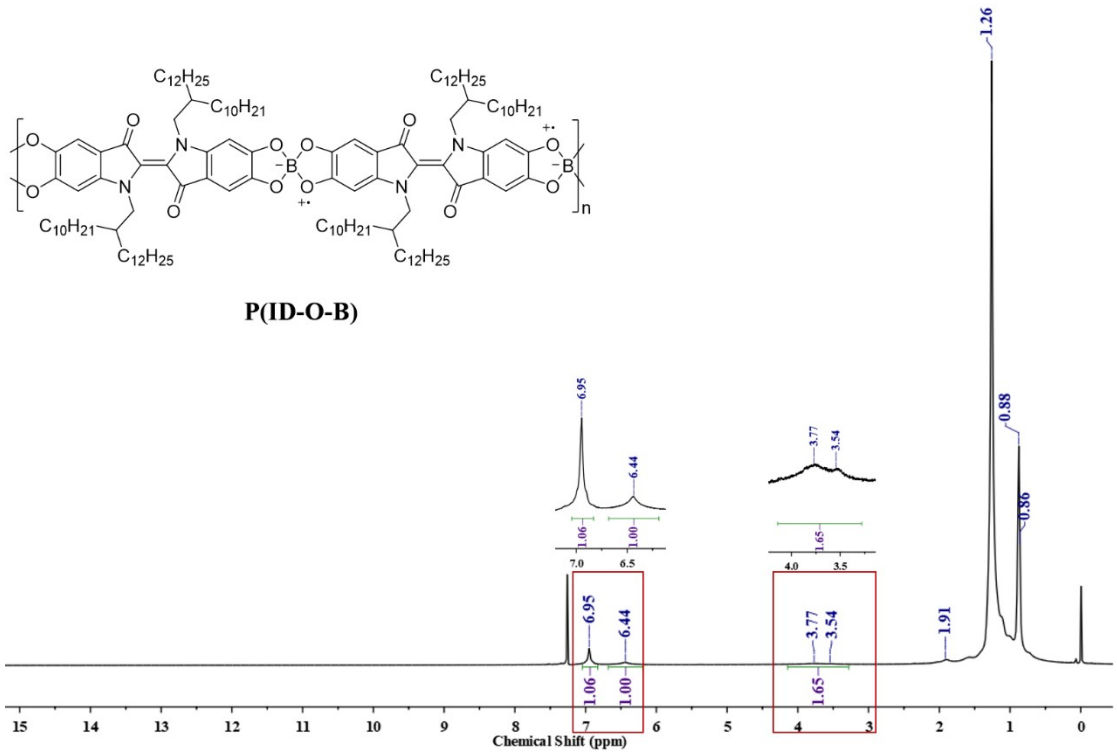

Figure S13. ^{1}H NMR spectrum (400 MHz) of P(ID-O-B) in $CDCl_3$.

Peak assignments are similar to the monomer, excepting that the phenolic proton is missing.

15. VT-EPR spectra of P(ID-O-B)

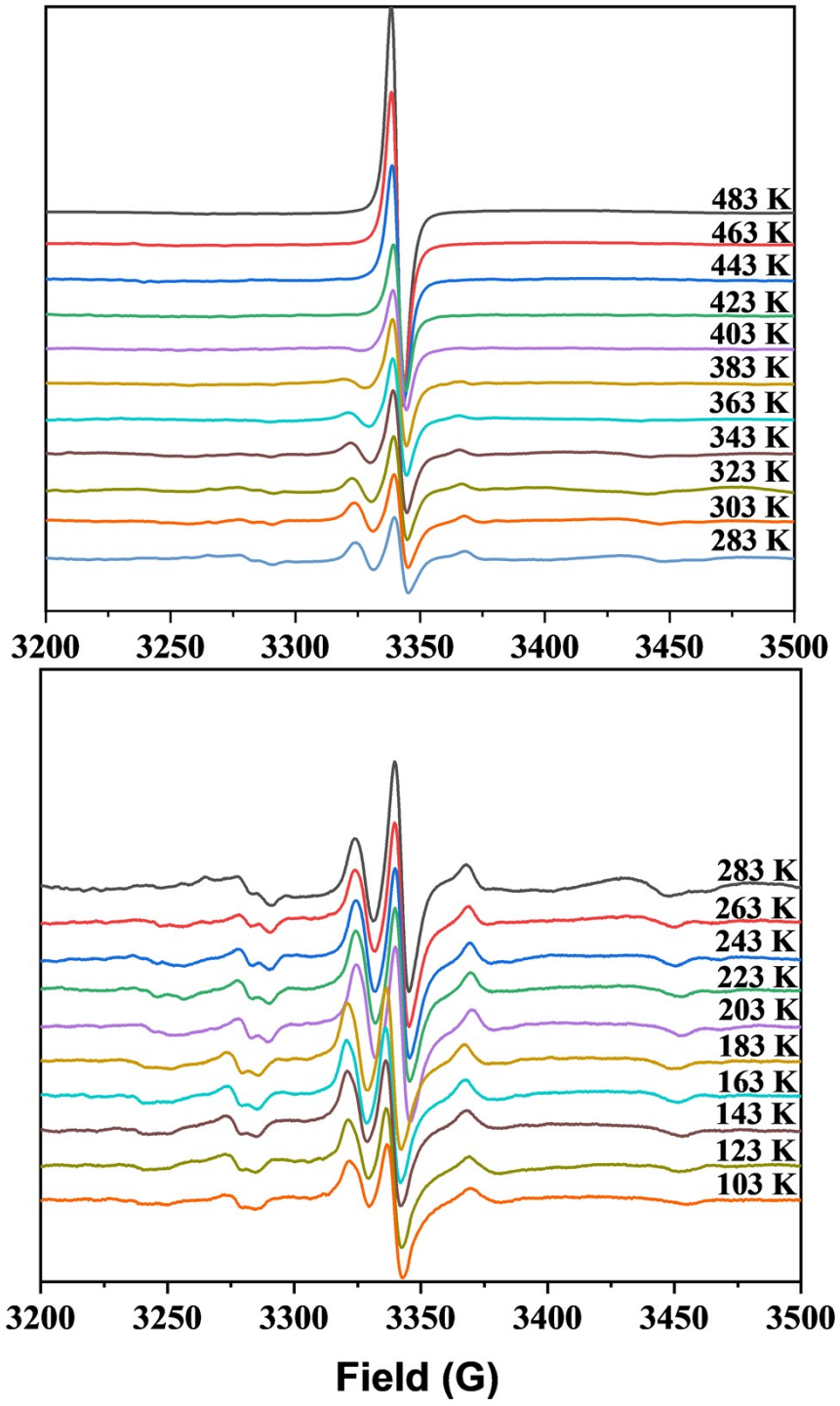

Figure S14. Temperature-dependency of EPR spectra of P(ID-O-B). Top figure: from 283 K to 483 K; Bottom figure: from 283 K to 103 K. For better view, the same intensity bar is used in each figure, but the intensity bars for the two figures are different.

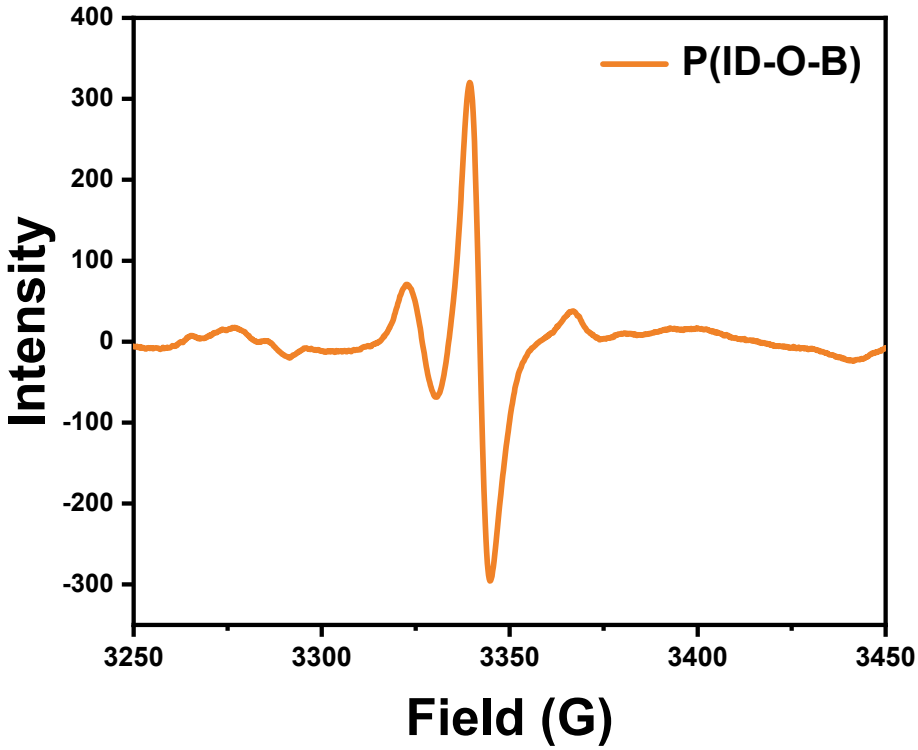

Figure S15. EPR spectrum of P(ID-O-B) after heating at 60 ℃ for 24 hours in an oxygen atmosphere at 4 MPa.

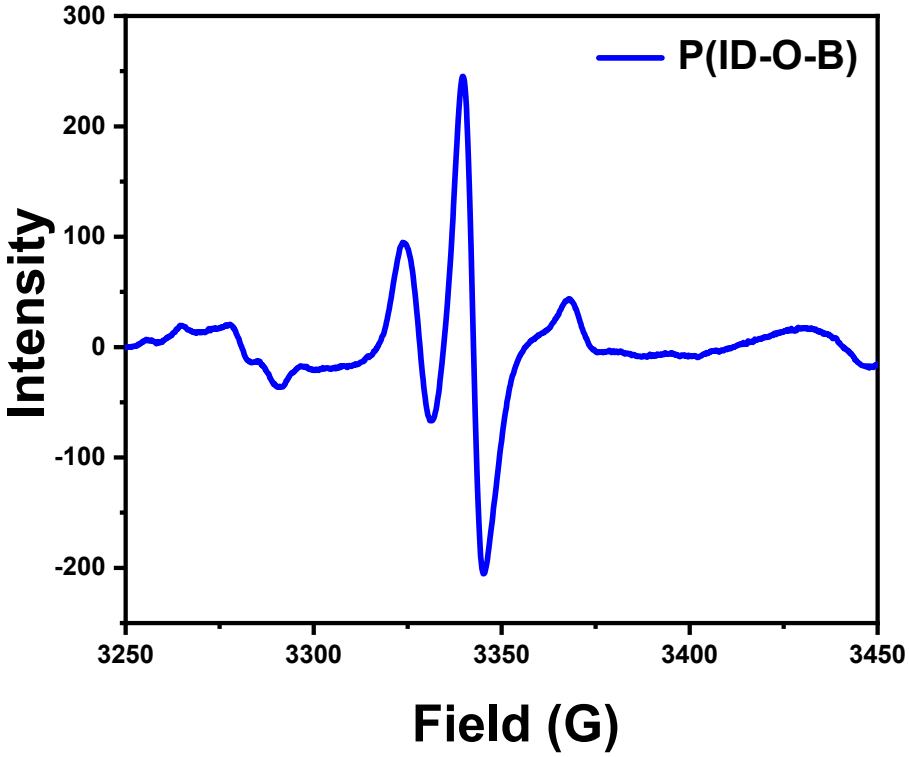

Figure S16. EPR spectra of P(ID-O-B) after 6 months in a normal environment.

16. ^{1}H NMR, ^{13}C NMR and high resolution mass spectra for all the other compounds

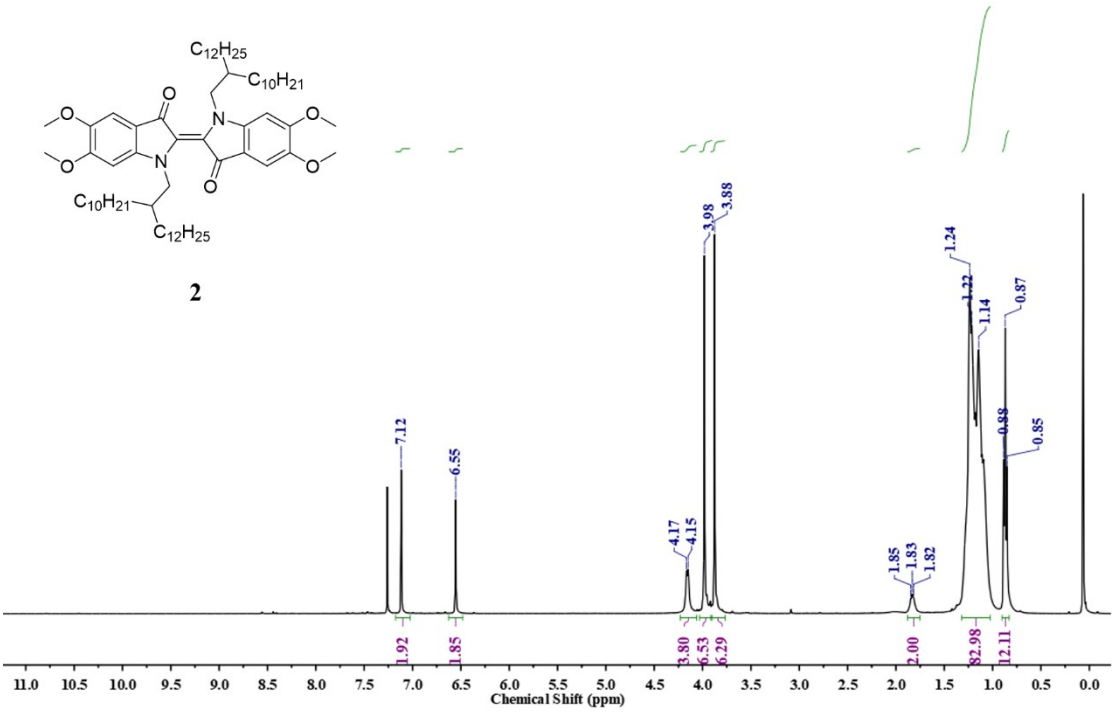

Figure S17. ^{1}H NMR spectrum (400 MHz) of compound 2 in $CDCl_3$.

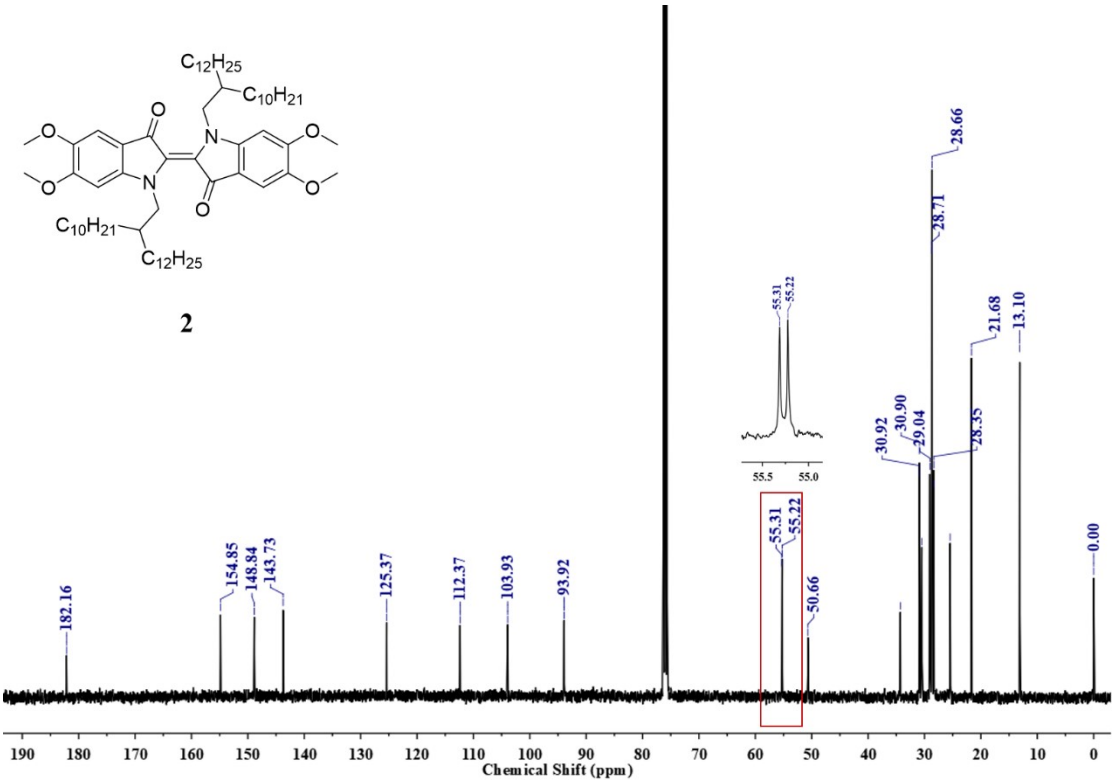

Figure S18. ^{13}C NMR spectrum (400 MHz) of compound 2 in $CDCl_3$.

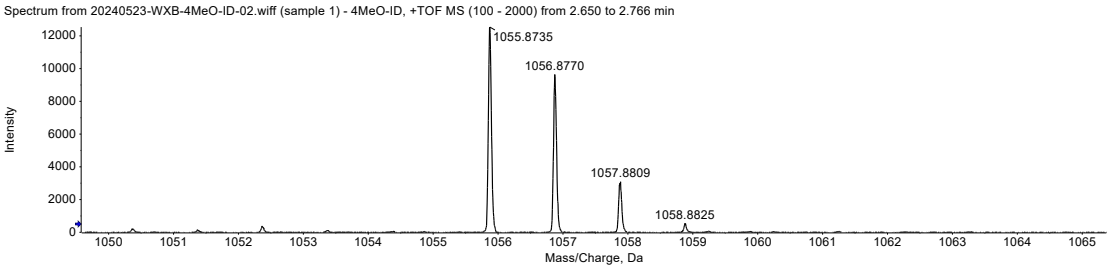

Figure S19. HR mass spectrum of compound 2 (4MeO-ID).

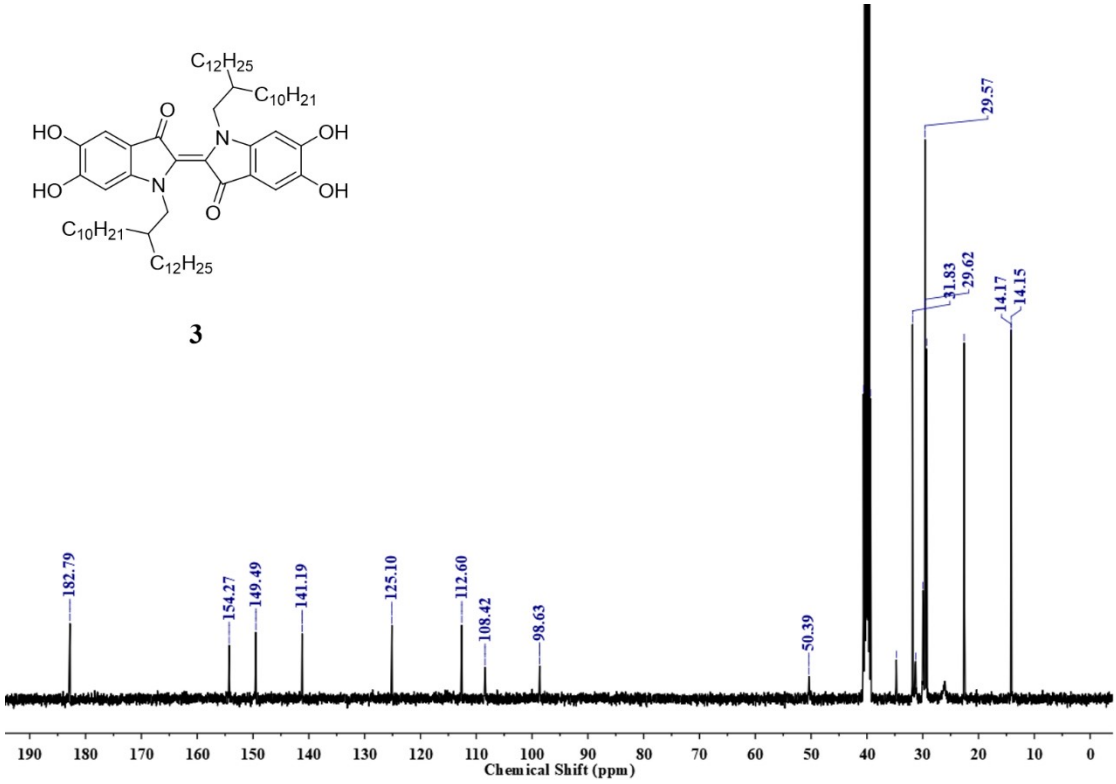

Figure S20. ^{13}C NMR spectrum (400 MHz) of compound 3 (4OH-ID) in DMSO-*d6*.

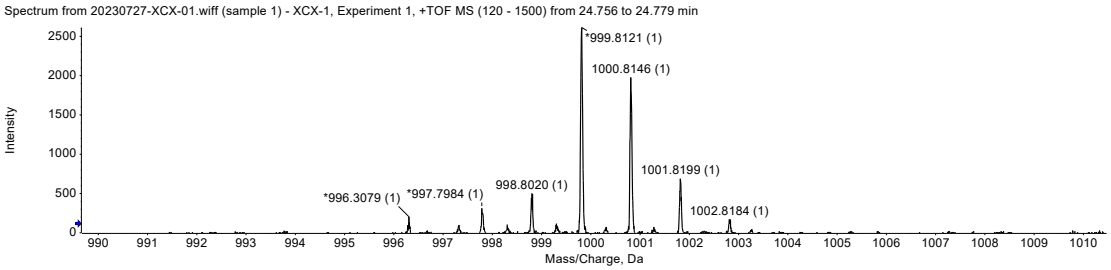

Figure S21. HR mass spectrum of compound 3 (4OH-ID).

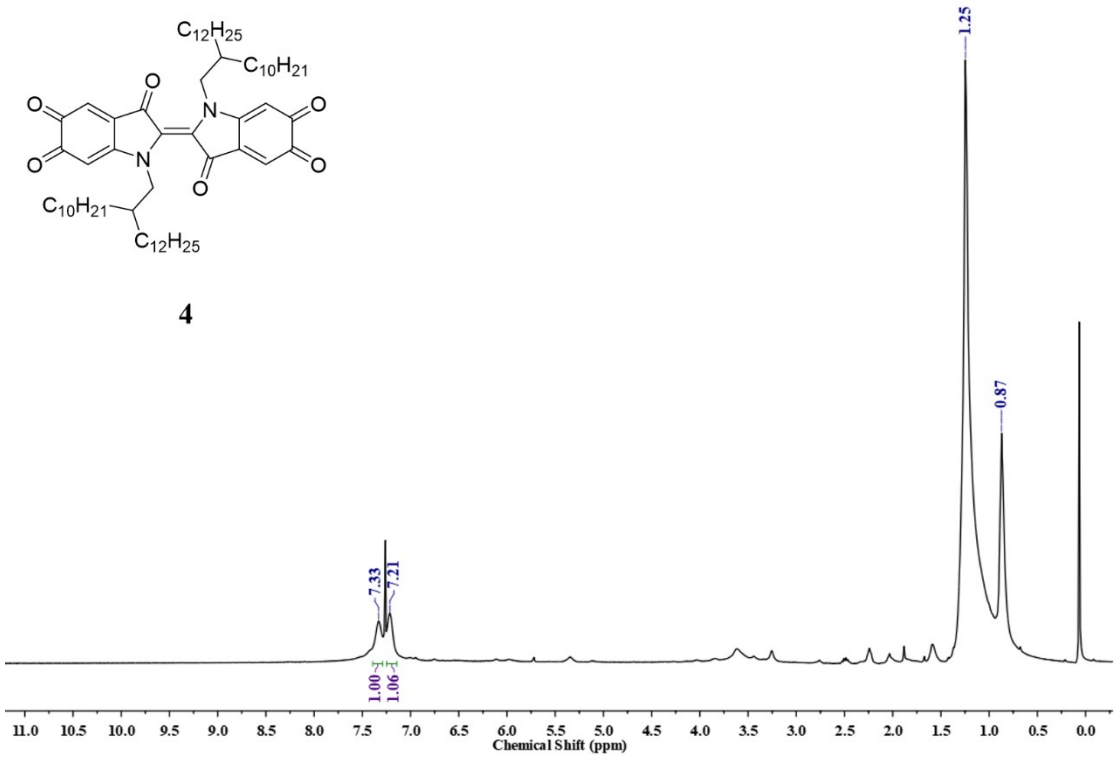

Figure S22. ^{1}H NMR spectrum (400 MHz) of compound 4 (4O-ID) in $CDCl_3$.

17. B-spectrum for P(ID-O-B)

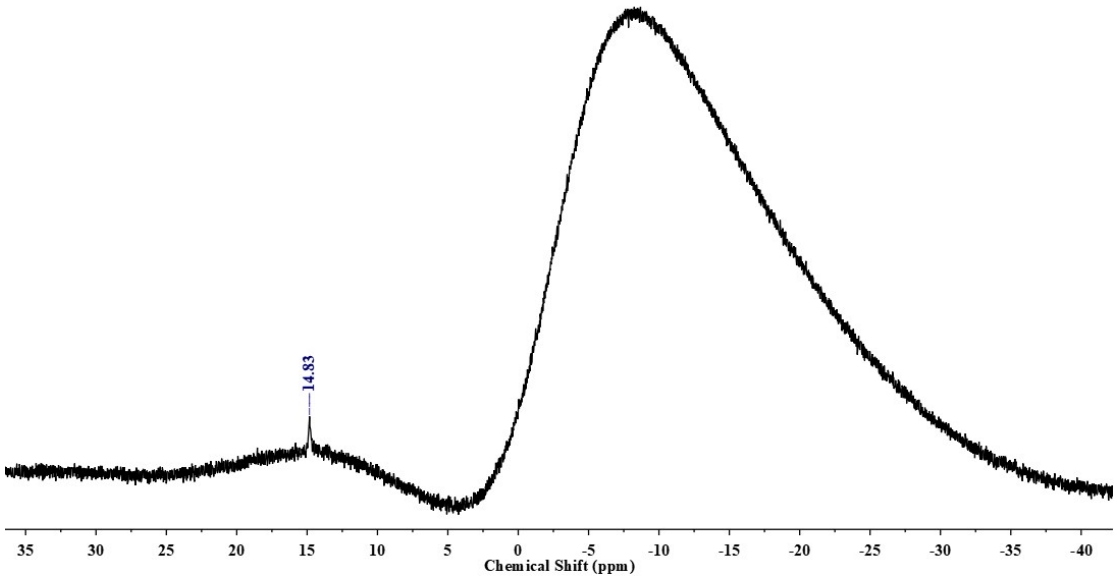

Figure S23. ^{11}B NMR spectrum (600 MHz) of P(ID-O-B) in $CDCl_3$ at 298 K.

18. Calculation Results

The optimization shows that the minimum of the close-shell singlet state lies 29.81 kcal/mol higher than the T_1 minimum, indicating that the lowest state is triplet. This is further confirmed by the spin density in Figure 2. In addition, the value of y is 0.843, indicating that the system is very close to the completed biradical character.

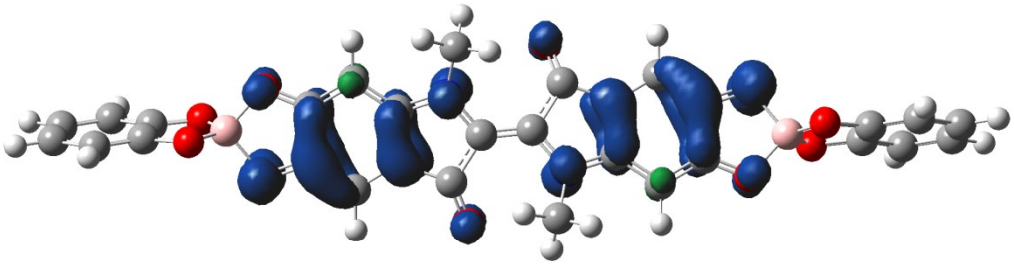

Figure S24. The spin density at Stru_T.

At Stru_T, the spin-flip TDDFT calculations show that the lowest singlet state displays the open-shell singlet character. Therefore, the energy order of these configurations are T_1 (triplet: 0 kcal/mol) < S_0 (open-shell singlet: 9.11 kcal/mol) < S_1 (close-shell singlet: 34.86 kcal/mol).

	Energy (kcal mol^{-1})
T1	set as 0
S0	9.11
S1	34.86

Cartesian coordinate of Stru_T (Angstrom).

atom	x	y	z
C	-11.856133	-0.200746	-0.320422
C	-11.643014	0.15733	-1.644694
C	-10.785364	-0.365572	0.567486
C	-9.519093	-0.158268	0.070842
C	-9.304896	0.201782	-1.260138
C	-10.349641	0.36661	-2.140152
O	-8.326294	-0.252369	0.724414
B	-7.338535	0.042217	-0.255986
O	-7.969485	0.347861	-1.492941
C	-5.152346	-0.750158	-0.106686
C	-5.167046	0.661752	0.27617
C	-4.014579	1.337004	0.654446
C	-2.853299	0.575767	0.63681
C	-2.835666	-0.809023	0.274728
C	-3.960371	-1.494322	-0.103749
N	-1.589698	0.979898	0.971715
C	-0.675218	-0.066731	0.829837
C	-1.454959	-1.287745	0.408415
C	0.675183	0.064908	0.829924
C	1.454795	1.286562	0.410121
C	2.835613	0.808273	0.2761
C	2.853397	-0.576984	0.636399
N	1.589799	-0.981743	0.970594
C	3.960275	1.494209	-0.101344
C	5.152361	0.750231	-0.10504
C	5.167215	-0.662172	0.27601
C	4.014779	-1.338085	0.653206
O	-1.019556	-2.381089	0.13858
O	1.019217	2.380146	0.141539
C	1.346125	-2.230752	1.675974
C	-1.345867	2.227745	1.67909
O	-6.326495	-1.151254	-0.414825
O	-6.359392	1.132561	0.198794
O	6.326491	1.151887	-0.412511
B	7.338639	-0.041742	-0.255399
O	6.35964	-1.1327	0.198234
C	9.304655	-0.199718	-1.260474
C	9.519274	0.158634	0.070899
C	10.785676	0.365595	0.567341
C	11.856151	0.202185	-0.321184
C	11.642618	-0.154201	-1.645846

C	10.349111	-0.363133	-2.141097
O	7.969195	-0.345783	-1.492972
O	8.326684	0.251608	0.72504
H	-12.868397	-0.356975	0.036668
H	-12.490595	0.277754	-2.310791
H	-10.938719	-0.644804	1.603425
H	-10.170182	0.646508	-3.171679
H	-4.044581	2.387967	0.907397
H	-3.938829	-2.542954	-0.373343
H	3.93863	2.543177	-0.369621
H	4.0449	-2.389367	0.904799
H	2.200132	-2.437964	2.322709
H	0.459057	-2.120467	2.296369
H	1.183063	-3.053275	0.983152
H	-2.200083	2.434332	2.325749
H	-0.459122	2.116114	2.299735
H	-1.182128	3.051236	0.987588
H	10.939355	0.643512	1.603585
H	12.868511	0.35819	0.035729
H	12.489979	-0.273543	-2.312417
H	10.169331	-0.641707	-3.172926

References:

1. Fukui, H. ; Nakano, M. ; Shigeta, Y.; Champagnes, B. Origin of the enhancement of the second hyperpolarizabilities in open-shell singlet transition-metal systems with metal–metal multiple bonds. *J. Phys. Chem. Lett.* **2011**, *2*, 2063.

2. Frisch, M. J.; Trucks, G. W.; Schlegel, H. B.; Scuseria, G. E.; Robb, M. A.; Cheeseman, J. R.; Scalmani, G.; Barone, V.; Mennucci, B.; Petersson, G. A. *et al.* Gaussian 16, Revision C.01, Gaussian Inc. Wallingford CT, USA, **2016**.

3. Shao, Y. H. ; Gan, Z. T.; Epifanovsky, E.; Gilbert, A. T. B. ; Wormit, M.; Kussmann, J.; Lange, A. W. ; Behn, A.; Deng, J.; Feng, X. T. *et al.* Advances in molecular quantum chemistry contained in the Q-Chem 4 program package. *Mol. Phys.* **2014**, *113*, 184.